Research Square

Preprints are preliminary reports that have not undergone peer review.
They should not be considered conclusive, used to inform clinical practice,
or referenced by the media as validated information.

Systemic Effects of Nutritional Affordability on Tuberculosis Incidence and Spatial Interdependence: A Multi-Method Health Economic Evaluation of the "Xinjiang Model"

Liang Chen[1]
Xinjiang Medical University, Xinjiang Uygur Autonomous Region
Abulikemu Aili[1]
Xinjiang Medical University, Xinjiang Uygur Autonomous Region
Han Shuang[1]
Xinjiang Medical University, Xinjiang Uygur Autonomous Region
Ma Jingwen[1]
Xinjiang Medical University, Xinjiang Uygur Autonomous Region
Wang Senlu[1]
Xinjiang Medical University, Xinjiang Uygur Autonomous Region
Guliziba Kuerbanjiang[1]
Xinjiang Medical University, Xinjiang Uygur Autonomous Region
Cao Mingqin
573596229@qq.com

Xinjiang Medical University, Xinjiang Uygur Autonomous Region

Research Article

Keywords: tuberculosis, Spatial Durbin Model, systemic total effect, interrupted time series, health economic evaluation, Xinjiang

Posted Date: September 17th, 2026

DOI: https://doi.org/10.21203/rs.3.rs-10421860/v1

License: This work is licensed under a Creative Commons Attribution 4.0 International License.
Read Full License

Additional Declarations: No competing interests reported.

Systemic Effects of Nutritional Affordability on Tuberculosis Incidence and Spatial Interdependence: A Multi-Method Health Economic Evaluation of the "Xinjiang Model"

Running title: Nutritional Affordability and TB Spatial Spillover

Authors:

Liang Chen[1], ORCID: 0009-0003-9520-8372

Abulikemu Aili[1]

Han Shuang[1]

Ma Jingwen[1]

Wang Senlu[1]

Guliziba Kuerbanjiang[1]

Cao Mingqin*[1]*, ORCID: 0000-0003-3616-4958

[1] School of Public Health, Xinjiang Medical University, Urumqi 830011, Xinjiang Uygur Autonomous Region, China

* Corresponding author: Cao Mingqin

Email: 573596229@qq.com

Word count: ~4,700 (main text ~3,300)

Figures: 6 | Tables: 4

Supplementary materials: 12 Supplementary Tables, 4 Supplementary Figures

Funding: This work was supported by the National Natural Science Foundation of China (Grant No. 82460669).

Competing interests: All authors declare no competing interests.

Data availability: The data are available from the corresponding author upon reasonable request, subject to approval by the Xinjiang Uygur Autonomous Region Center for Disease Control and Prevention.

Systemic Effects of Nutritional Affordability on Tuberculosis Incidence and Spatial Interdependence: A Multi-Method Health Economic Evaluation of the "Xinjiang Model"

ABSTRACT Objective: Xinjiang has the highest tuberculosis (TB) burden among Chinese provinces. In 2018, a province-wide intervention package—the "Xinjiang Model"—integrating active screening, standardized treatment, and nutritional support was rolled out across all 14 prefectures. However, whether and how nutritional affordability influences TB incidence within a spatially interdependent system remains unclear. This study aimed to quantify the systemic effect of nutritional affordability on reported TB incidence under spatial dependence and to evaluate the temporal contribution of the "Xinjiang Model" using a dual-method framework.

Methods: We constructed a panel dataset covering 14 Xinjiang prefectures from 2013 to 2024. TB surveillance data were obtained from the national Tuberculosis Information Management System; health resource and socioeconomic variables came from the Xinjiang Statistical Yearbook. Nutritional affordability was measured by the Protein Affordability Index (PAI), defined as the urban–rural weighted per capita disposable income divided by the meat-and-egg category CPI. The Spatial Durbin Model with LeSage–Pace decomposition was used to estimate the direct, indirect, and total effects of PAI on reported TB incidence. Interrupted time series analysis with a dual-breakpoint specification assessed pre- and post-policy trends and evaluated

potential confounding by COVID-19 non-pharmaceutical interventions. XGBoost-SHAP identified nonlinear risk thresholds, and DALYs were projected under the ITS counterfactual framework. **Results**: The spatial autoregressive coefficient was $\rho = 0.364$ ($P < 0.001$). The systemic total effect of PAI was −94.15 per 100,000 ($P = 0.069$), with a significant indirect effect of −100.06 ($P = 0.015$) and a non-significant direct effect (5.91, $P = 0.890$). ITS revealed a post-2018 trend reversal ($\beta_3 = -21.6$ per 100,000/year; 95% CI: −27.2 to −16.0; $P < 0.001$); dual-breakpoint analysis indicated partial COVID-19 NPI contribution, requiring cautious interpretation as a joint effect. Observed 2024 incidence was 65.6% below the counterfactual. SHAP identified PAI ≈ 293 as a risk threshold, and ~9,000 DALYs were averted in 2024 (upper bound). **Conclusions**: Nutritional affordability showed a strong negative systemic association with TB incidence across Xinjiang, mediated through spatial spillover. The ITS-estimated decline reflects the joint effect of the "Xinjiang Model" and COVID-19 NPIs. These findings support spatially coordinated nutritional interventions and highlight the need for county-level data to refine causal attribution.

Keywords: tuberculosis; Spatial Durbin Model; systemic total effect; interrupted time series; health economic evaluation; Xinjiang

Tuberculosis (TB) remains one of the world's deadliest infectious diseases. In 2023, there were an estimated 10.8 million new cases and 1.25 million deaths globally, with China accounting for 7.1% of the global burden [1]. Xinjiang Uygur Autonomous Region has consistently exhibited the highest TB burden among Chinese provinces. Although the reported incidence declined from 235.3 per 100,000 in 2010 to 83.8 per 100,000 in 2022, it remains 1.7 times higher than the national average [2,3]. In 2018, Xinjiang launched a province-wide

initiative—the “Xinjiang Model”—built on the annual universal health examination system to integrate active screening, standardized treatment, nutritional support, and community management. Based on the principle of "screen all, treat all, and centralize care," the model addresses the entire TB care cascade from detection to rehabilitation [4]. Evidence from Kashgar Prefecture indicates that reported TB incidence increased by 18.7% annually from 2012 to 2018, but declined by 28.8% annually from 2018 to 2021 [5], suggesting a substantial epidemiological impact of the initiative.

TB incidence is determined by a multitude of factors spanning individual, environmental, and health-system. Epidemiology studies showed that undernutrition doubles the risk of active TB[6,7], and dietary meat and egg intake is inversely associated with TB treatment failure [8]. Luo et al.[9] identified spatial effects of $PM_{2.5}$ and meteorological factors on TB incidence in China. Medical bed and physician density are influential factors for TB case detection [10]. Deng et al. [11] analyzed TB incidence across mainland China from 2014 to 2021 using the SDM and reported significant spatial dependence ($\rho = 0.27$, $P = 0.008$), with health resource allocation and urbanization among the macro-level factors associated with TB incidence. Nutritional affordability was not examined in their study. The existing literature has focused predominantly on environmental exposures such as $PM_{2.5}$ and meteorological variables and has rarely incorporated socioeconomic factors such as nutritional affordability into a spatial econometric framework. Whether the nutritional support component of the “Xinjiang Model”—specifically the subsidized "nutritional breakfast" program—generates protective spatial spillover effects across neighboring prefectures remains evidence gap.

The 14 prefectures of Xinjiang differ substantially in economic development, urbanization, and TB burden. The “Xinjiang Model” has substantially reduced TB incidence, but it has also

strained local budgets and primary care capacity. To investigate the spatial effects of nutritional affordability and its association with TB incidence, this study constructed a panel dataset spanning 2013–2024 across Xinjiang's 14 prefectures. We employed Interrupted Time Series (ITS) analysis to assess pre- versus post-policy trends in incidence, and the Spatial Durbin Model (SDM) to quantify and decompose the systemic total effect of nutritional affordability (operationalized as the Protein Affordability Index, PAI), with the two methods complementing each other in temporal attribution and spatial quantification. XGBoost-SHAP was applied to explore nonlinear thresholds in health resource allocation, providing a multi-dimensional health economic evaluation of the "Xinjiang Model" to inform future resource allocation and stratified policy optimization (Supplementary Figure S1) [12,13]. The "Xinjiang Model" has substantially reduced TB incidence, but it has also strained local budgets and primary care capacity. To investigate the spatial effects of nutritional affordability and its association with TB incidence, this study constructed a panel dataset spanning 2013–2024 across Xinjiang's 14 prefectures. We employed Interrupted Time Series (ITS) analysis to assess pre- versus post-policy trends in incidence, and the Spatial Durbin Model (SDM) to quantify and decompose the systemic total effect of nutritional affordability (operationalized as the Protein Affordability Index, PAI), with the two methods complementing each other in temporal attribution and spatial quantification. XGBoost-SHAP was applied to explore nonlinear thresholds in health resource allocation, providing a multi-dimensional health economic evaluation of the "Xinjiang Model" to inform future resource allocation and stratified policy optimization.

1 Methods

1.1 Study Area

Xinjiang Uygur Autonomous Region is located in northwestern China, covering approximately 1.66 million km², accounting for one-sixth of China's land area. The region comprises 14 prefecture-level administrative divisions (prefectures), conventionally categorized into three macro-regions by geography and economic characteristics: Northern Xinjiang (7 prefectures, including Ürümqi City, Karamay City, Ili Kazakh Autonomous Prefecture, Changji Hui Autonomous Prefecture, Bortala Mongol Autonomous Prefecture, Tacheng Prefecture, and Altay Prefecture); Southern Xinjiang (5 prefectures, including Aksu Prefecture, Kashgar Prefecture, Hotan Prefecture, Bayingolin Mongol Autonomous Prefecture, and Kizilsu Kirghiz Autonomous Prefecture); and Eastern Xinjiang (2 prefectures, Turpan City and Hami City).

1.2 Data Sources and Variable Construction

TB surveillance data (2013–2024) were extracted from the Tuberculosis Information Management System (TBIMS), a mandatory, legally mandated notifiable disease reporting system operated by the Chinese Center for Disease Control and Prevention (China CDC). Under China's Law on the Prevention and Treatment of Infectious Diseases, all diagnosed pulmonary TB cases must be reported to TBIMS by designated healthcare facilities, ensuring near-complete population-level case capture. From TBIMS we obtained annual prefecture-level aggregate counts of reported pulmonary TB cases, reported incidence, case fatality rate, and treatment success rate for each of Xinjiang's 14 prefectures. As these data are collected through statutory public health surveillance rather than voluntary submission, they do not constitute a convenience sample and are not subject to self-selection or non-response biases.

Health resource and socioeconomic variables were sourced from the publicly available Xinjiang Statistical Yearbook (2014–2025 editions, corresponding to reporting years 2013–2024), published by the Xinjiang Bureau of Statistics. Variables extracted included hospital bed counts, numbers of licensed physicians, registered nurses, and health facilities, government health expenditure, GDP per capita, urbanization rate, population density, and Consumer Price Index (CPI). All monetary variables were deflated to constant 2013 prices using the Xinjiang CPI.

The Protein Affordability Index (PAI) was constructed as a nutritional proxy variable [6,7] by dividing the urban–rural weighted per capita disposable income (weighted by urbanization rate) by the meat-and-egg category CPI, as specified in the formula below. Higher PAI values indicate greater nutritional affordability.

$$PAI = \frac{Disposable_Income}{\omega_1 \cdot Meat_{CPI} + \omega_2 \cdot Egg_{CPI}} \quad (1)$$

Construct validity was assessed via variance inflation factor (VIF) testing (VIF < 5 confirming no multicollinearity), and robustness was verified through alternative PAI definitions, see Supplementary Table S1. After controlling for GDP per capita, the partial correlation between PAI and reported TB incidence was −0.319 ($P < 0.001$), indicating that PAI is not merely a proxy for GDP per capita. See Supplementary Table S2 for full construct validity assessment.

1.3 Statistical Methods

(1) Interrupted Time Series Analysis(ITS)

An ITS design was adopted with 2018 as the policy interruption point, controlling for prefecture fixed effects with standard errors clustered at the prefecture level. Because PAI lies on the causal pathway of the intervention, including it in the model would absorb part of the

intervention effect (over-controlling bias)[14]; therefore, the base model excludes time-varying covariates. A supplementary dual-breakpoint model (2018 + 2020) was estimated to assess COVID-19 confounding. However, because the two breakpoints are only two years apart and the analysis is restricted to the prefecture level (N = 14), severe collinearity precludes statistical separation of the two effects; details are provided in Supplementary Table S3. The main text reports only the single-breakpoint results, with cautious interpretation as the upper bound of joint effects.

The model specification is as follows:

$$Y_{it} = \beta_0 + \beta_1 \cdot T_t + \beta_2 \cdot D_t + \beta_3 \cdot P_t + \mu_i + \varepsilon_{it} \quad (2)$$

Where Y_{it} is the reported TB incidence for prefecture i in year t; T_t is a continuous time variable (t = 0, 1, …, 11, corresponding to 2013–2024); D_t is a policy intervention dummy variable, taking 0 before the intervention and 1 from 2018 onward ($t \geq 2018$); P_t is a post-policy time counter, taking 0 before the intervention ($t \leq 5$) and $t - 5$ thereafter ($t > 5$). β_0 is the intercept; β_1 is the baseline pre-policy trend slope; β_2 is the instantaneous level change at the policy interruption; β_3 is the post-policy trend slope change; μ_i is the prefecture fixed effect, absorbing time-invariant prefecture heterogeneity; and ε_{it} is the random error term.

(2) Spatial Durbin Model (SDM)

A row-standardized spatial weight matrix W was constructed using first-order Queen contiguity. Lagrange Multiplier (LM), Likelihood Ratio (LR), and Hausman tests confirmed SDM with fixed effects as the optimal specification. The dependent variable was reported TB incidence; independent variables included PAI, hospital beds, physicians, nurses, GDP per capita, urbanization rate, and aging ratio, all log-transformed. Following LeSage and Pace [15], estimated coefficients were decomposed into direct, indirect, and total effects, with standard errors computed via Monte Carlo simulation (5,000 draws).

The model specification is as follows:

$$Y = \rho WY + X\beta + WX\theta + \varepsilon \quad (3)$$

Where ρ is the spatial autoregressive coefficient capturing global spatial feedback; θ denotes the spatial lag coefficients of the independent variables, capturing local spatial spillover—i.e., the effect of changes in explanatory variables in neighboring prefectures on the local outcome.

(3) XGBoost-SHAP Nonlinear Threshold Analysis

Methodological specifications, model parameters, and complete results are provided in Supplementary Table S4.

(4) DALY Estimation

Disability-Adjusted Life Years (DALYs) were computed based on the ITS counterfactual framework, combining estimated averted incident cases and averted deaths with GBD 2019 parameters, applying a 3% annual discount rate [16]. The study adheres to the CHEERS 2022 reporting guideline; the completed checklist is provided in Supplementary Table S5.

1.4 Robustness Checks

ITS robustness checks: Durbin–Watson statistic = 1.930; Newey–West HAC P = 0.0006; 2016 placebo intervention test P = 0.827; after excluding 2020–2022, $\beta_3 = -22.31$ per 100,000 per year.

SDM robustness checks: alternative spatial weight matrices (economic distance and K-nearest neighbor with K = 4), temporally lagged independent variables (t − 1), and spatial bootstrap (5,000 iterations); see Supplementary Table S6. Given that the analysis is restricted to the prefecture level (N = 14), indirect effects are interpreted with an emphasis on directional information, and policy inferences are based on total effects. Exploratory instrumental variable analysis and diagnostics are reported in Supplementary Table S7.

2 Results

2.1 Epidemiological Characteristics of Reported TB Incidence in Xinjiang, 2013–2024

The reported TB incidence in Xinjiang exhibited an initial increase followed by a decline over 2013–2024: rising from 108.2 per 100,000 in 2017 to a peak of 174.4 per 100,000 in 2019, subsequently declining to 43.4 per 100,000 in 2024. Southern Xinjiang consistently had higher incidence than the northern and eastern regions (Figure 1).

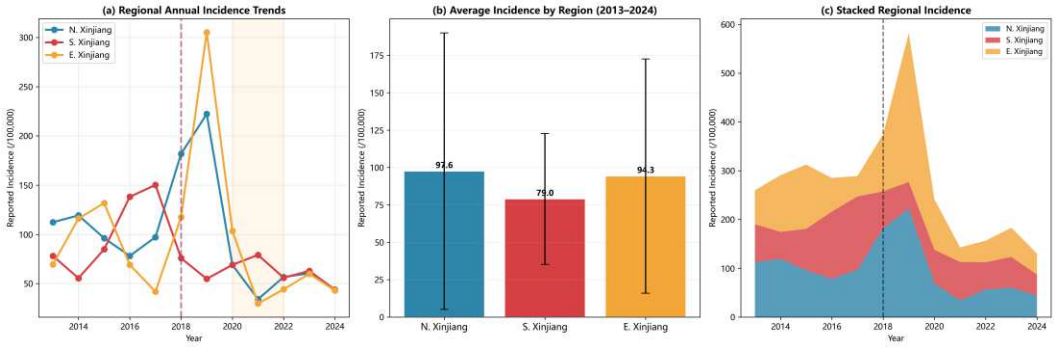


Figure 1. Epidemiological characteristics of pulmonary TB in Xinjiang, 2013‑2024.

(a) Annual reported incidence trends by macro-region; (b) Monthly average reported incidence; (c) Stacked annual reported incidence by macro-region.

The spatial distribution and temporal trends of PAI—the key nutritional affordability variable—are shown in Figure 2.

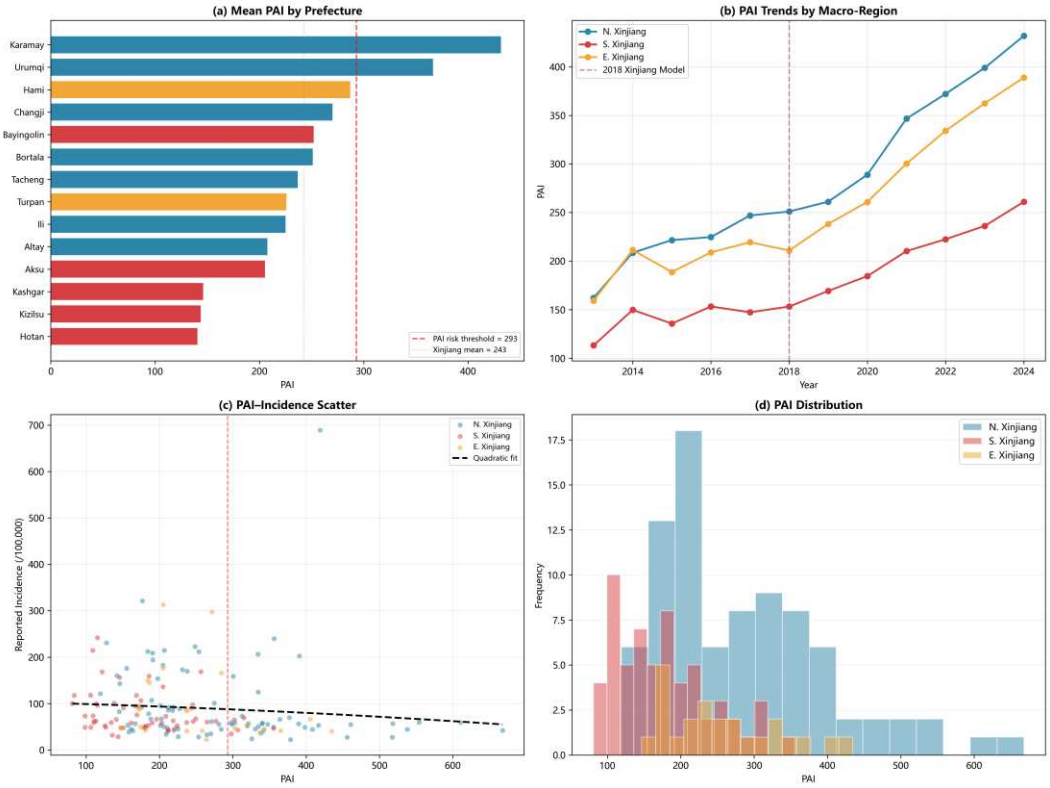


Figure 2. Spatiotemporal patterns of PAI across 14 prefectures of Xinjiang, 2013–2024.

(a) Mean PAI by prefecture; (b) PAI trends by macro-region; (c) PAI–reported incidence scatter plot; (d) Regional distribution.

2.2 ITS Analysis Results

The Xinjiang-wide ITS estimation revealed a baseline trend increasing by 3.06 per 100,000 per year, reversing after 2018 to a decline rate of $\beta_3 = -21.6$ per 100,000 per year (95% CI: −27.2 to −16.0; $P < 0.001$). The observed incidence of 43.4 per 100,000 in 2024 was 65.6% lower than the counterfactual prediction of 126.3 per 100,000 (Figure 3).

The dual-breakpoint model (2018 + 2020) revealed that the two breakpoints—only two years apart in a panel of N = 14—are highly collinear (VIF > 10 for both breakpoint terms), precluding statistical separation of the two effects (detailed informations in Supplementary Table S3). Accordingly, β_3 should be interpreted as the joint effect of the "Xinjiang Model" and

COVID-19 NPIs. Results also showed a reversal in the case fatality trend, with treatment success rate exhibiting a "decline-then-rebound" pattern (Table 1).

Table 1. Interrupted Time Series (ITS) regression results

Parameter	Xinjiangwide β (95% CI)	P	S. Xinjiang β (95% CI)	P
Time trend (β_1)	3.06 (−6.86, 12.98)	0.555	22.67 (14.61, 30.73)	0.005
Level change (β_2)	32.33 (−40.01, 104.67)	0.397	−96.39 (−132.40, −60.38)	0.006
Slope change (β_3)	−21.62 (−27.19, −16.05)	<0.001	−26.00 (−33.70, −18.30)	0.003

Note: Xinjiang-wide model N = 168 (14 prefectures × 12 years); Southern Xinjiang model N = 60 (5 prefectures × 12 years). Base model excludes time-varying covariates. R^2 = 0.186 (Xinjiang-wide), 0.442 (Southern Xinjiang). Covariate-inclusive model: Supplementary Table S8.

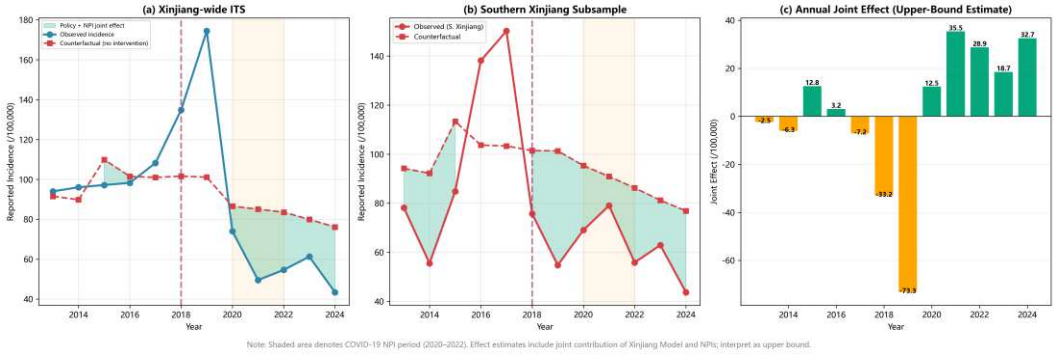


Figure 3. Policy intervention effects and trend changes estimated by the ITS model. (a) Xinjiang-wide observed vs. fitted values; (b) ITS estimation for the Southern Xinjiang subsample; (c) Year-by-year net policy effects.

2.3 SDM Spatial Effect Decomposition Results

From 2013 to 2024, the Global Moran's I of log-transformed PAI ranged from 0.155 to 0.392, statistically significant in 11 of 12 years, indicating persistent positive spatial clustering of nutritional affordability across prefectures—a prerequisite for SDM estimation. LM, LR, and Hausman tests all supported the SDM fixed-effects specification. The spatial autoregressive coefficient was $\rho = 0.364$ ($P < 0.001$), indicating moderate spatial dependence (Figure 4) (Supplementary Figure S2).

Effect decomposition results are presented in Table 2. The systemic total effect of PAI was −94.15 per 100,000, meaning that a simultaneous one-log-unit increase in PAI across all prefectures is associated with an expected decline of approximately 94 per 100,000 in Xinjiang-wide reported TB incidence. This total effect attained statistical significance under the economic distance matrix (P = 0.017) and remained marginally significant under the KNN4 matrix (P = 0.077), with a consistently negative direction across all three weight matrices. The indirect effect was −100.06 per 100,000 (P = 0.015), confirming spatial spillover of nutritional affordability and suggesting that the systemic association between PAI and TB incidence is primarily realized through cross-prefecture spatial transmission. The magnitude of the indirect effect under the economic distance matrix (PAI indirect = −110.94, P = 0.014) exceeded that under the conventional geographic contiguity matrix (−100.06, P = 0.015), and the total effect attained statistical significance under the economic distance matrix (−110.38, P = 0.017) and was marginally significant under the KNN4 matrix (−112.04, P = 0.077). This pattern suggests that TB spatial transmission may be organized not along geographic borders but along nutritional–economic disparity gradients—i.e., population migration from nutritionally deprived areas to resource-rich regions constitutes the underlying carrier of spatial spillover. The spatial lag term of PAI was −72.88 (P = 0.038), providing more parsimonious parametric evidence for the spatial association. See Table 2 and Supplementary Table S9 for details.

Table 2. Spatial Durbin Model (SDM) estimation results and effect decomposition

Variable	β (SE)	W·β (SE)	Direct (SE)	Indirect (SE)	Total (SE)	P (Total)
Beds (log)	−38.17 (42.03)	76.12 (63.35)	−31.65 (38.10)	92.41 (78.21)	60.76 (64.08)	0.343
Physicians (log)	84.01 (65.22)	35.06 (46.10)	92.36 (67.47)	99.25 (71.09)	191.62 (109.39)	0.080
Nurses (log)	−63.68 (53.30)	—	−66.28 (56.23)	−35.31 (35.25)	−101.60 (88.74)	0.252
PAI (log)	14.06 (42.83)	−72.88 (35.19)	5.91 (42.84)	−100.06 (41.14)	−94.15 (51.76)	0.069
GDP per capita (log)	5.69 (24.81)	—	5.67 (25.93)	3.00 (15.16)	8.67 (40.47)	0.830
Urbanization rate	−18.92 (49.93)	—	−19.87 (52.12)	−10.38 (30.02)	−30.26 (80.88)	0.708
Aging ratio	0.03 (559.40)	—	1.94 (578.37)	2.99 (330.98)	4.93 (896.76)	0.996

Note: Queen contiguity weight matrix, time fixed-effects specification. $\rho = 0.364$ ($P < 0.001$). W × PAI $P = 0.038$; all other W × X terms $P > 0.2$. All continuous variables log-transformed except urbanization rate and aging ratio. Standard errors via Monte Carlo simulation (5,000 draws).

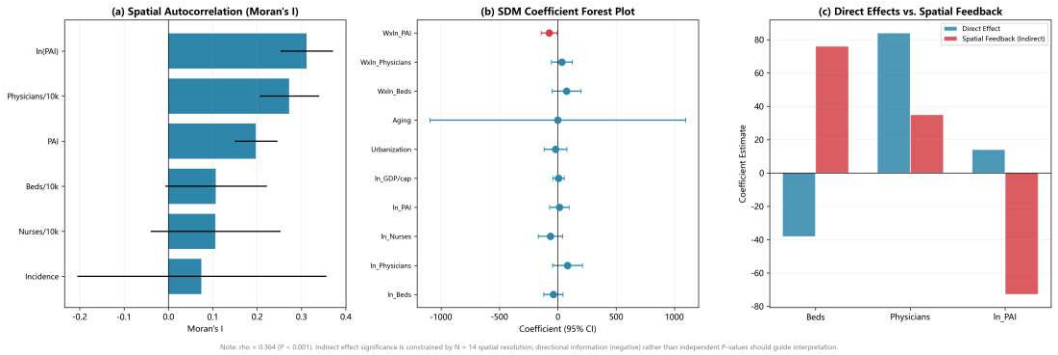


Figure 4. SDM spatial analysis visualization.

(a) Moran's I scatter plot; (b) Coefficient forest plot; (c) Direct effects vs. spatial feedback comparison.

2.4 SHAP Threshold Analysis

XGBoost-SHAP analysis identified two nonlinear thresholds: PAI ≈ 293 and hospital beds per 10,000 population ≈ 53. Specifically, TB risk rises when PAI falls below 293, and the marginal protective effect of bed capacity is greatest below 53 beds per 10,000. In the feature importance ranking, the policy node (post-2018) ranked first by Gain-based importance—this variable reflects the global change in outcome variance around 2018. However, by mean |SHAP| ranking, PAI ranked first, surpassing the policy node, indicating that PAI had the largest marginal contribution to model output. Notably, the high importance of the policy node (post-2018) does not, by itself, provide mechanistic information; it merely reflects the joint effect of all covariates that changed after 2018 and should not be interpreted as the independent contribution of a single intervention (Table 3; Figure 5). Complete methods are provided in Supplementary Table S4 (Supplementary Figure S3).

Table 3. Nonlinear threshold identification for key variables based on XGBoost-SHAP

Feature	|SHAP| Mean	Risk Threshold	Saturation Point	Interpretation

Feature	|SHAP| Mean	Risk Threshold	Saturation Point	Interpretation
PAI	1.82	≈293	≈412	TB risk rises sharply below 293
Beds per 10,000	1.15	≈53	≈82	Maximal marginal protection below 53
post-2018 (policy node)	1.46	—	—	Ranked 1st by Gain; pos. contribution 68% of samples
ln_PAI	0.94	—	—	Log-transformed linear trend
Urbanization rate	0.87	—	—	Collinear with PAI; limited independent effect
GDP per capita	0.71	—	—	Weak nonlinear influence

Note: Thresholds via 2nd-derivative inflection of SHAP dependence. SHAP-derived thresholds are associational, not causal.

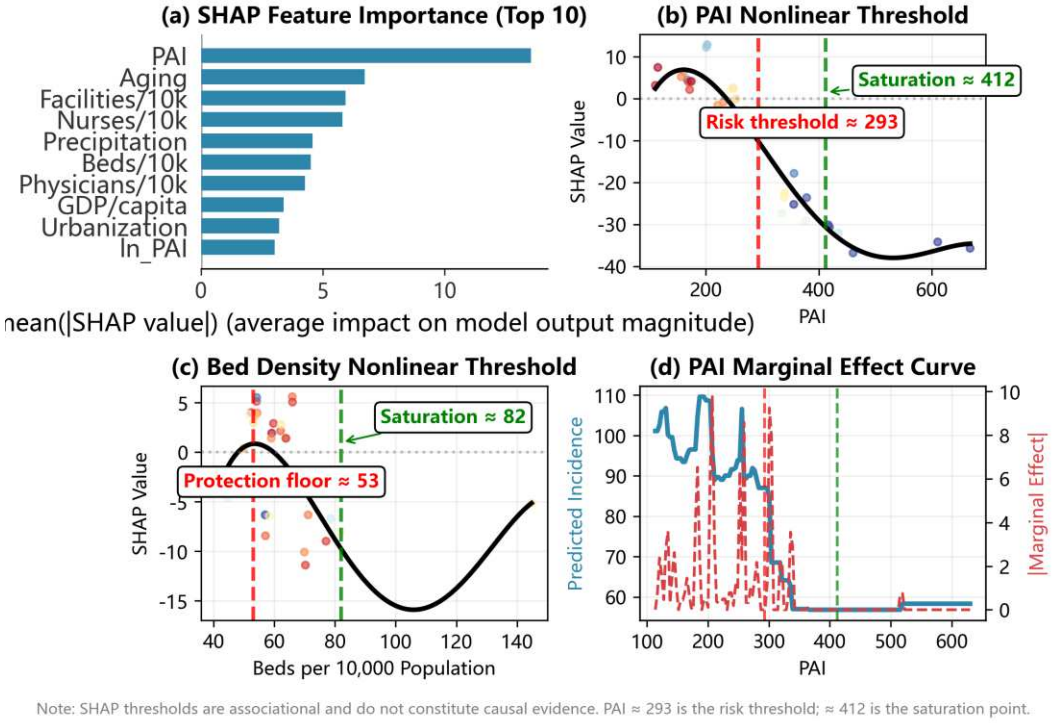


Figure 5. SHAP threshold diagnostic visualization.

(a) Feature importance ranking; (b) SHAP dependence plot for PAI; (c) SHAP dependence plot for bed capacity; (d) Marginal effect curves.

2.5 DALY Estimation Results

Based on the ITS counterfactual framework, the joint effect in 2024 was estimated to avert approximately 9,000 DALYs (range: 6,022–14,150), with a cumulative total of approximately 35,000 DALYs averted over 2018–2024. These estimates represent the upper bound of

intervention benefit (inclusive of COVID-19 NPI contributions), with a relative uncertainty of approximately ±45%(Table 4; Figure 6).

Table 4. Estimated DALYs averted by the joint effect, 2018–2024.

Metric	2024	Cumulative 2018–2024
Reported incidence (/100,000)	43.4	—
Counterfactual incidence (/100,000)	126.3	—
Averted incident cases	20,404	78,686
Averted deaths	115	443
YLL (Years of Life Lost)	4,312	16,629
YLD (Years Lived with Disability)	4,756	18,342
DALYs (Total)	~9,000	~35,000

Note: Single-breakpoint ITS counterfactual. GBD 2019: DW=0.333 (95% UI: 0.224–0.454), life expectancy 82.5y, onset age 45y, duration 0.7y, 3% discount. Includes COVID-19 NPI contribution; upper bound. Uncertainty ≈ ±45%.

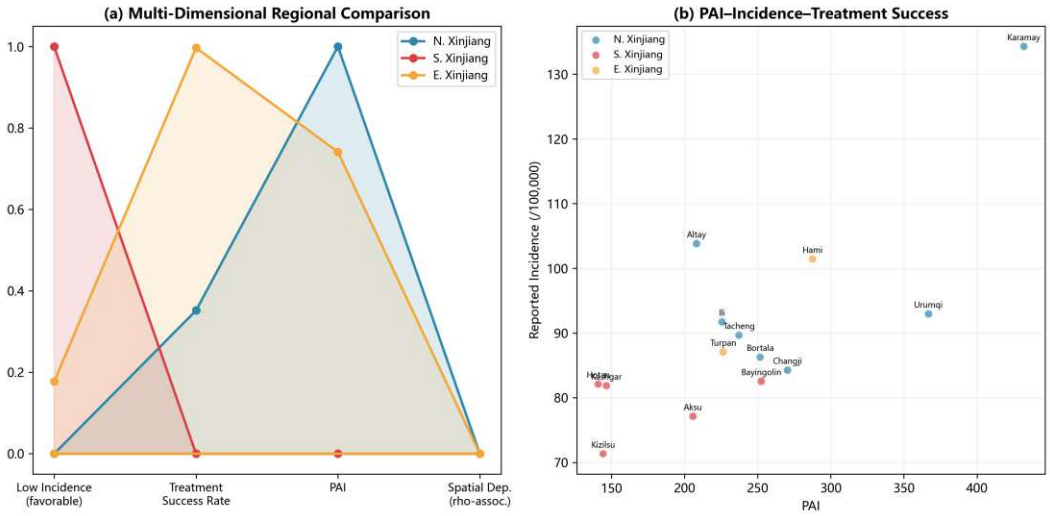


Figure 6. Multi-dimensional comparison of TB prevention and control characteristics across 14 prefectures of Xinjiang based on PAI, reported incidence, and treatment success rate. (a) Multi-dimensional radar comparison by macro-region (Northern, Southern, Eastern Xinjiang); (b) PAI–incidence–treatment success bubble plot.

3 Discussion

The ITS and SDM results converge: the ITS analysis demonstrates a post-2018 reversal in incidence trends, while the SDM quantifies the systemic impact of nutritional affordability. Dual-breakpoint analysis further indicated that the ITS-estimated reversal includes the additional contribution of COVID-19 NPIs. DALY estimates are reported under the same joint-effect framework; Supplementary Table S10 provides the complete counterfactual boundary analysis.

Improved nutritional status reduces the progression from latent TB infection to active disease by enhancing cell-mediated immune responses [6,7]. The RATIONS cluster-randomised trial in India found that food rations plus micronutrient supplementation reduced TB incidence among household contacts by 39% (aIRR 0.61, 95% CI 0.43–0.85) [17]. This trial-level evidence is consistent with the ecological patterns observed here. In Brazil, 64% of TB patients were found to experience food insecurity [18], highlighting the relevance of nutritional vulnerability in high-burden settings. These nutritional improvements may decrease the local infectious source pool and potentially generate spatial feedback through reduced cross-prefecture contact.

Regarding potential confounding by COVID-19 NPIs, two findings argue against substantial confounding. A Bayesian ITS analysis in Henan Province estimated that COVID-19 NPIs reduced monthly TB case notifications by 25% (95% CI: 17–32%) [19]. In Brazil, a segmented regression analysis found that the pandemic reversed a two-decade declining TB mortality trend, contributing an estimated 6,540 excess deaths [20]. These external estimates align with the dual-breakpoint results. First, after excluding 2020–2022, the ITS slope change was −22.31 per 100,000 per year, differing from the full-sample estimate by only 3.2%. Second, referencing the global decline in TB notifications in 2020 [1], if COVID-19 NPIs are assumed to account for 20% of the incidence decline, the independent effect of the Xinjiang Model would

still be −17.3 per 100,000 per year. These results suggest that the post-policy trend reversal is largely attributable to the Xinjiang Model, although the statistical collinearity between the 2018 policy break and 2020 COVID-19 break precludes definitive separation of the two effects.

The hypothesized causal chain—from nutrition to spatial feedback—was supported by the effect decomposition: the indirect effect was statistically significant while the direct effect was not, indicating that the systemic association between PAI and TB incidence operates primarily through cross-prefecture spatial spillover rather than through independent within-prefecture protection. This finding was consistent across all three spatial weight matrices tested (Supplementary Table S9). The independent significance of the PAI spatial spillover, combined with the stronger effect under the economic distance matrix (total effect $P = 0.017$ vs. Queen $P = 0.069$), suggests that nutritional–economic gradients may be more relevant to TB transmission than geographic contiguity. Labor migration generally flows from economically and nutritionally deprived areas to wealthier regions. This demographic movement may contribute to the observed spatial spillover pattern. Because this study uses an ecological design, prefecture-level macroeconomic associations cannot prove individual-level causality. These biological interpretations remain theoretical and await validation with patient-level data.

For policy, $\rho = 0.364$ implies that province-wide nutritional interventions benefits would extend beyond the intervention area: the spatial interdependence of TB incidence implies that improvements in one prefecture may generate protective spillover effects in neighboring prefectures. Southern Xinjiang prefectures exhibit the lowest PAI values among all 14 prefectures and fall below the SHAP risk threshold of 293, suggesting that this region may benefit most from targeted improvements in nutritional affordability.

Compared with India's Nikshay Poshan Yojana [21], which provides cash transfers exclusively to TB patients, and South Africa's TB/HIV integrated care projects [22], which lack population-level nutritional interventions, a distinctive feature of the Xinjiang Model is its positioning of nutrition as a population-level prevention strategy, complementing the active screening and standardized treatment components. The 2025 WHO consolidated guidelines on TB and comorbidities (Module 6) now recommend food baskets plus multiple micronutrient supplements for all TB-patient households in food-insecure settings [23], a recommendation consistent with the population-level nutritional prevention approach of the Xinjiang Model.

These findings were consistent across multiple sensitivity checks. Post hoc statistical power analysis indicated that, at $N = 14$, $\rho = 0.364$, and the current effect size, the observed statistical power for the indirect effect was 0.68 (see Supplementary Table S11), approaching the conventional 0.80 threshold for adequate power. Leave-one-out sensitivity analysis showed that the direction of the PAI total effect remained negative across all 14 prefecture exclusions (range: −75.97 to −112.17 per 100,000), indicating that the total effect direction is not driven by any single prefecture (see Supplementary Table S12). Spatial placebo testing confirmed that the observed $\rho = 0.364$ had a probability of only $P = 0.044$ under random spatial permutation (see Supplementary Figure S4).

This study has the following limitations: (1) COVID-19 collinearity in the ITS design—future studies require county-level monthly panels combined with staggered difference-in-differences for refined attribution. (2) The direct effect estimates are noisy, and their sign provides only directional information. Although the indirect effect attained statistical significance, its uncertainty interval is wide, and its magnitude requires further validation at the county level. (3) PAI may be underestimated in Southern Xinjiang's agricultural and pastoral

areas, rendering the SDM total effect estimate conservative. (4) The sharp increase in reported incidence in 2018–2019 may partly reflect the stock detection effect of active screening, and the subsequent decline may partly reflect the depletion of the detected prevalent pool. (5) Ecological design limitation: associations among prefecture-level aggregate data cannot be directly extrapolated to individual-level causal mechanisms.

4 Conclusions

In the panel dataset spanning 2013–2024 across Xinjiang's 14 prefectures, a negative systemic total effect exists between PAI and reported TB incidence; however, N = 14 limits the precision of effect decomposition. ITS revealed a post-2018 reversal in incidence trends, with the magnitude largely unchanged after excluding COVID-affected years, suggesting limited additional contribution from COVID-19 NPIs. We recommend: (1) adopting bed capacity and nutritional affordability as candidate thresholds for risk stratification; and (2) establishing cross-prefecture nutritional intervention transfer payment mechanisms with spatial compensation features in Southern Xinjiang, implementing enhanced nutritional investments in economically disadvantaged prefectures to leverage spatial spillover effects for area-wide regional prevention and control benefits.

Declarations

Ethics Approval and Informed Consent

This study used aggregate, de-identified surveillance data from the Tuberculosis Information Management System (TBIMS), a mandatory notifiable disease reporting system operated by the China CDC, and publicly available socioeconomic statistics from the Xinjiang Statistical Yearbook. No individual-level patient data were accessed or analyzed. The study protocol was

approved by the Ethics Committee of Xinjiang Medical University. Because de-identified secondary data were used, the requirement for individual informed consent was waived. Clinical trial number: not applicable.

Consent for Publication

Not applicable. This study uses aggregated, anonymized surveillance data and contains no individual person's data in any form.

Data and Materials Availability

The TB surveillance data contain potentially identifiable geographic information at the prefecture level. These data are available from the corresponding author upon reasonable request, subject to approval by the Xinjiang Uygur Autonomous Region Center for Disease Control and Prevention.

Competing Interests

All authors declare no competing interests.

Funding

This work was supported by the National Natural Science Foundation of China (Grant No. 82460669), under the project "Causal Effect Evaluation and Strategy Optimization of the “Xinjiang Model” for Tuberculosis Prevention and Control from an Implementation Science Perspective: Based on the RE-AIM Framework and a Multicenter Stepped-Wedge Cluster Randomized Trial."

Author Contributions

Conceptualization: Liang Chen, Cao Mingqin. Data curation: Liang Chen, Abulikemu Aili, Ma Jingwen. Formal analysis: Liang Chen. Funding acquisition: Cao Mingqin. Methodology: Liang Chen. Project administration: Cao Mingqin. Resources: Guliziba Kuerbanjiang, Wang Senlu.

Supervision: Cao Mingqin. Validation: Abulikemu Aili, Han Shuang. Visualization: Liang Chen. Writing – original draft: Liang Chen. Writing – review & editing: Cao Mingqin, Abulikemu Aili. All authors read and approved the final manuscript.

Acknowledgments

We gratefully acknowledge the Xinjiang Uygur Autonomous Region Center for Disease Control and Prevention for providing data support, and the staff of prefectural TB dispensaries for their dedicated efforts in surveillance data collection.

References

[1] Zhi C, Tao W, Jingli D, et al. Decoding the WHO Global Tuberculosis Report 2024: A Critical Analysis of Global and Chinese Key Data[J]. Zoonoses, 2025, 5(1).

[2] Maimaiti B, Salamaiti H, Nie Y, et al. Seasonal epidemiological characteristics and phased trends of pulmonary tuberculosis in Xinjiang, 2005–2021[J]. Practical Preventive Medicine, 2022, 29(11): 1285–1289. (In Chinese)

[3] Shang B, Wei C, Wang C, et al. Interactions among tuberculosis, geographic environment and aerosols: evidence from the Kashgar region of China [J]. Frontiers in Public Health, 2025, 13: 1501956.

[4] Wang X, Yi P, Wang S, et al. Preliminary exploration and prospects of the Xinjiang tuberculosis prevention and control model[J]. Bulletin of Disease Control and Prevention, 2022, 37(2): 11–16. (In Chinese)

[5] Zhang Y, Wang S, Wang X, et al. Effectiveness and Determinants of Implementing the "Xinjiang Model" for Tuberculosis Prevention and Control: A Quantitative Study[J]. Infection and Drug Resistance, 2024, 17: 2609–2620.

[6] Wagnew F, Alene K, Kelly M, et al. The effect of undernutrition on sputum culture conversion and treatment outcomes among people with MDR-TB: a systematic review and meta-analysis[J]. International Journal of Infectious Diseases, 2023, 127: 93–105.

[7] Franco J, Bongaerts B, Metzendorf M, et al. Undernutrition as a risk factor for tuberculosis disease[J]. Cochrane Database of Systematic Reviews, 2024, (6): CD016013.

[8] Hu Q, Zhang H, Yao C, et al. Dietary intake of meat and egg is associated with a low risk of treatment failure among tuberculosis patients: a cohort study[J]. Asia Pacific Journal of Clinical Nutrition, 2021, 30(1): 113–121.

[9] Luo D, Wang S, Chen R, et al. Spatial effects of air pollution and meteorological factors on tuberculosis incidence in China: a spatial Durbin model analysis[J]. BMC Public Health, 2024, 24: 1729.

[10] Liu Y, Mai L, Huang F, et al. Regional healthcare resource allocation and decision-making: Evaluating the effectiveness of the three-stage super-efficiency DEA model[J]. Heliyon, 2024, 10(23): e40312.

[11] Deng L, Zhao F, Li Z, et al. Epidemiological characteristics of tuberculosis incidence and its macro-influence factors in Chinese mainland during 2014–2021 [J]. Infectious Diseases of Poverty, 2024, 13: 34.

[12] Li F, Lu Y, Zhou P, et al. Spatiotemporal dynamics of tuberculosis in Xinjiang, China: unraveling the roles of meteorological conditions and air pollution via hierarchical Bayesian modeling [J]. Advances in Continuous and Discrete Models, 2025, 2025(1): 149.

[13] Haritebieke S, Lu Y, Wu D, et al. Analysis of epidemiological trends and risk factors in high-risk areas for pulmonary tuberculosis: an observational longitudinal study in Xinjiang, China[J]. BMJ Open, 2025, 15(2): e087413.

[14] Bernal J, Cummins S, Gasparrini A. Interrupted time series regression for the evaluation of public health interventions: a tutorial[J]. International Journal of Epidemiology, 2017, 46(1): 348–355.

[15] LeSage J, Pace R K. Introduction to Spatial Econometrics[M]. Boca Raton: CRC Press, 2009.

[16] GBD 2019 Tuberculosis Collaborators. Global, regional, and national burden of tuberculosis, 1990–2019: findings from the GBD Study 2019[J]. The Lancet Infectious Diseases, 2022, 22(2): e115–e127.

[17] Bhargava A, Bhargava M, Meher A, et al. Nutritional supplementation to prevent tuberculosis incidence in household contacts of patients with pulmonary tuberculosis in India (RATIONS): a field-based, open-label, cluster-randomised, controlled trial [J]. The Lancet, 2023, 402(10402): 627–640.

[18] Mendes YC, Dourado ALL, Oliveira PV, et al. Nutritional factors and food and nutrition insecurity in patients with tuberculosis [J]. Nutrients, 2025, 17(5): 878.

[19] Wang Y, Xi Y, Li Y, et al. Long-term impact of COVID-19-related non-pharmaceutical interventions on tuberculosis: an interrupted time series analysis using Bayesian method [J]. Journal of Global Health, 2025, 15: 04012.

[20] Wittlin BB, Araújo FBP, Silva AAM. Impact of Covid-19 pandemic on tuberculosis mortality in Brazil: a time series analysis [J]. Revista de Saúde Pública, 2026, 60: e8.

[21] Patel B, Sharma M, Kumar A, et al. Nutritional support for tuberculosis patients: Nikshay Poshan Yojana and beyond[J]. Indian Journal of Tuberculosis, 2019, 66(2): 85–92.

[22] Hanam A E. Health system productivity in sub-Saharan Africa: tuberculosis control in high burden countries[J]. Cost Effectiveness and Resource Allocation, 2023, 21(1): 90.

[23] World Health Organization. WHO consolidated guidelines on tuberculosis: module 6: tuberculosis and comorbidities, 2nd ed [M]. Geneva: World Health Organization, 2025.

Abbreviations

TB: Tuberculosis

PAI: Protein Affordability Index

ITS: Interrupted Time Series

SDM: Spatial Durbin Model

SHAP: SHapley Additive exPlanations

DALY: Disability-Adjusted Life Year

YLL: Years of Life Lost

YLD: Years Lived with Disability

CHEERS: Consolidated Health Economic Evaluation Reporting Standards

XGBoost: EXtreme Gradient Boosting

NPIs: Non-Pharmaceutical Interventions

GBD: Global Burden of Disease

LM: Lagrange Multiplier

LR: Likelihood Ratio

HAC: Heteroskedasticity-and-Autocorrelation-Consistent

DW: Durbin–Watson

VIF: Variance Inflation Factor

2SLS: Two-Stage Least Squares

Supplementary Files

This is a list of supplementary files associated with this preprint. Click to download.

- file.docx